Active Control of Neoclassical Tearing Modes toward Stationary High-Beta Plasmas in JT-60U

A. Isayama 1), N. Oyama 1), H. Urano 1), T. Suzuki 1), M. Takechi 1), N. Hayashi 1), K. Nagasaki 2), Y. Kamada 1), S. Ide 1), T. Ozeki 1) and the JT-60 team 1)

1) Japan Atomic Energy Agency, Naka, Ibaraki 311-0193, Japan
2) Institute of Advanced Energy, Kyoto University, Uji, Kyoto 611-0011, Japan

e-mail contact of main author: isayama.akihiko@jaea.go.jp

Abstract. Results from active control of neoclassical tearing modes (NTMs) with electron cyclotron current drive (ECCD) in JT-60U are described. Evolution of an NTM with the poloidal mode number $m = 3$ and the toroidal mode number $n = 2$ has been suppressed by ECCD inside the $q = 1$ surface in the co-direction, showing the possibility of the coexistence of sawtooth oscillations and a small-amplitude $m/n = 3/2$ NTM without large confinement degradation. Stabilization of an $m/n = 2/1$ NTM by ECCD at the $q = 2$ surface has been demonstrated with a small value of the ratio of the current density driven by electron cyclotron (EC) wave to the local bootstrap current density ($J_{EC}/J_{BS} \sim 0.5$). Also, dependence of the stabilization effect on ECCD location has been investigated in detail, and it has been clarified that an $m/n = 2/1$ NTM can be completely stabilized with the misalignment of the ECCD location less than about half of the island width, and that the $m/n = 2/1$ NTM is destabilized with the misalignment comparable to the island width. Time-dependent, self-consistent simulation of magnetic island evolution using the TOPICS code has shown that the above stabilization and destabilization of an $m/n = 2/1$ NTM are well reproduced with the same set of coefficients of the modified Rutherford equation. The TOPICS simulation has also clarified that EC wave power required for complete stabilization can be significantly reduced by narrowing the ECCD width.

1. Introduction

In a fusion reactor, plasma operation with a high fraction of bootstrap current is expected in order to reduce externally driven current. For example, bootstrap current fraction of $\sim 30\%$ is expected in the ITER hybrid scenario [1]. In such plasmas, however, neoclassical tearing modes (NTMs) would be excited. Since the NTMs degrade the plasma performance and sometimes cause a disruption, it is critically important to establish a scenario to control the NTMs. Stabilization of NTMs by electron cyclotron current drive (ECCD) at the mode rational surface, which is typically located at half of the minor radius, has been successfully performed in ASDEX-U [2], DIII-D [3] and JT-60U [4], and methods for NTM control have been steadily developed and improved since then.

Among various possible mode numbers, NTMs with $m/n = 3/2$ and $2/1$ should be controlled since the degradation of the plasma performance can be large and intolerable. Here, m and n are the poloidal and toroidal mode numbers, respectively. In JT-60U, an $m/n = 3/2$ NTM was completely stabilized by using a real-time NTM stabilization system, where the detection of the mode location and the optimization of the injection angle of electron cyclotron (EC) wave are performed in real time [5]. Also, preemptive NTM stabilization, where EC wave is injected to the anticipated mode location before the mode onset, has been shown effective [6]. In addition, a high-beta plasma with the normalized beta $\beta_N \sim 3$ was sustained for 5 times longer than the energy confinement time by suppressing NTMs [7].

This paper describes results from active control of NTM with ECCD in JT-60U. In Section 2, control of a $3/2$ NTM by central ECCD is shown. This operational scenario is quite different from the conventional NTM stabilization in that the ECCD location is far outside the mode rational surface. Section 3 shows stabilization of a $2/1$ NTM by ECCD at the mode rational surface. Dependence of stabilization effect on ECCD location has been investigated in detail. And, in Section 4, results from simulation of a $2/1$ NTM using the TOPICS code are described focusing on the effects of ECCD location and ECCD width on NTM stabilization.

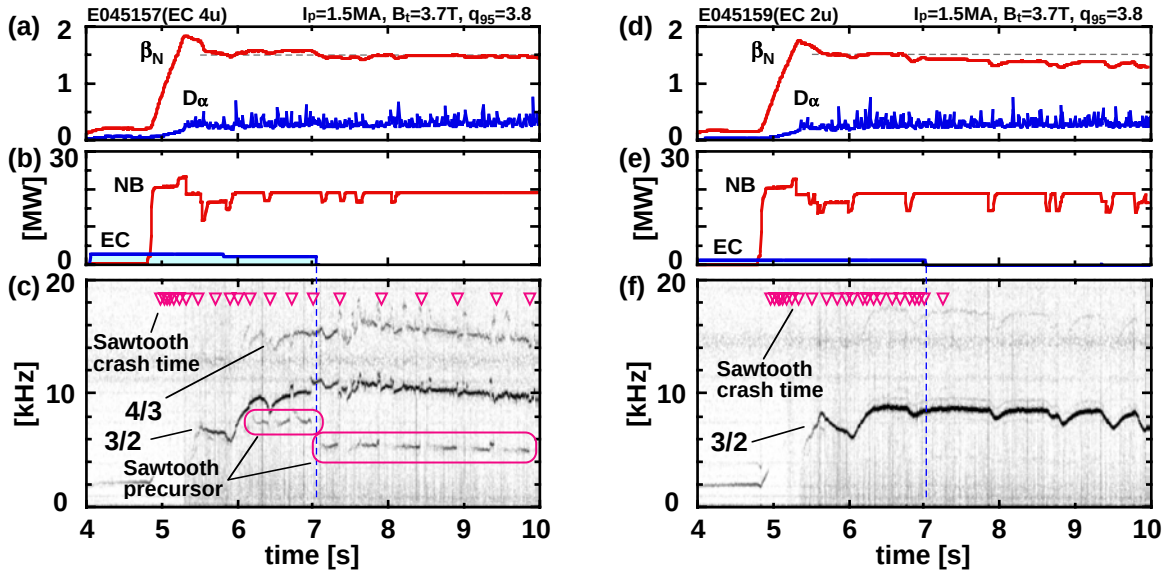

FIG. 1. Typical discharges of control of a 3/2 NTM by central co-ECCD for the cases of 4-unit ECCD ((a)–(c)) and 2-unit ECCD ((d)–(f)). (a) and (d): Normalized beta and intensity of D_α signal, (b) and (e): injection power of NB and EC wave, (c) and (f): frequency spectrum of magnetic perturbations. Triangles in (c) and (f) indicate the time of a sawtooth crash.

2. Control of Evolution of a 3/2 NTM by Central Co-ECCD

Sawtooth oscillations are considered beneficial in controlling heat and particles at the core region. In JT-60U, it was demonstrated that the amplitude and period of sawtooth oscillations can be actively controlled by optimizing the location and direction of the ECCD. In particular, ECCD in the same direction as the existing plasma current (co-ECCD) inside the sawtooth inversion radius can enhance sawtooth oscillations [8]. However, in relation to NTMs, sawtooth oscillations are considered harmful since a large sawtooth crash can trigger an NTM even at a low-β regime (β is the ratio of the plasma pressure to the magnetic pressure). Thus, it is important to clarify the effect of sawtooth oscillations on an NTM and to develop a scenario for controlling the NTM.

In JT-60U, effects of central co-ECCD on a 3/2 NTM have been investigated aiming at modifying the current profile at the center and also aiming at destabilizing sawtooth oscillations. Typical discharge is shown in Figs. 1(a)–(c). Plasma parameters are as follows: plasma current $I_\mathrm{p} = 1.5$ MA, toroidal field $B_\mathrm{t} = 3.7$ T, and safety factor at the 95% flux surface $q_{95} = 3.8$. In this discharge, EC wave, whose frequency and power are 110 GHz and 2.4 MW, respectively, is injected from $t = 4.0$ s prior to the main heating by neutral beams (NBs). A ray-tracing Fokker-Planck code shows that the peak of the EC-driven current is located at 0.1 in the volume-averaged minor radius ρ (see Fig. 2), and that the total driven current is 130 kA. By this injection, sawtooth oscillations appear from $t = 4.97$ s while no sawtooth is observed without EC wave injection. An NTM with $m/n = 3/2$ appears at $t \sim 5.5$ s when β_N reaches 1.6 (poloidal beta $\beta_\mathrm{p} = 1.2$). The 3/2 mode is located at $\rho \sim 0.4$. Electron temperature profile measured with electron cyclotron emission (ECE) diagnostic shows that at $t \sim 5$ s inversion radius of sawtooth oscillations is located at $\rho \sim 0.15$. The inversion radius gradually increases in time and reaches $\rho = 0.22$ at $t = 7$ s. As shown in the triangles in Fig. 1(c), the period of the sawtooth oscillations also increases in time and reaches about 500 ms at $t = 7.8$ s. The sawtooth period is maintained even after the turnoff of the EC wave injection. As the inversion radius and the period increase, precursor of sawtooth crash can become recognized in the frequency spectrum as shown in Fig. 1(c). It can be also seen that when the precursor become visible the mode frequency is modulated

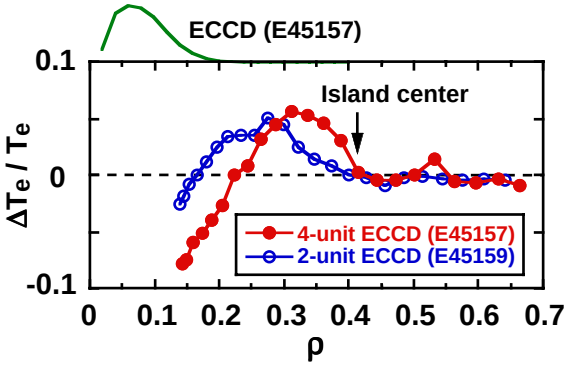

FIG. 2. Profiles of change in electron temperature during a sawtooth crash for the cases of 4-unit ECCD and 2-unit ECCD.

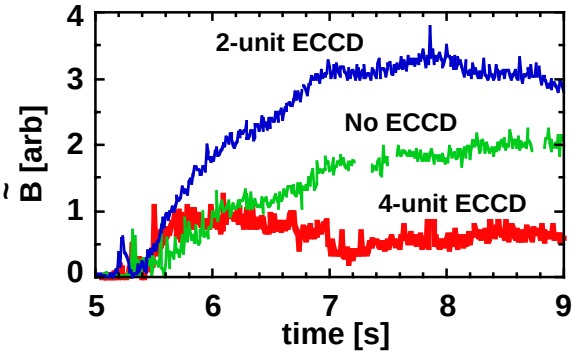

FIG. 3. Temporal evolution of amplitude of magnetic perturbations in the frequency range of 5.5 to 13 kHz for the cases of no ECCD, 2-unit ECCD, and 4-unit ECCD are shown.

by a sawtooth crash. The rapid change in the frequency of the $3/2$ mode cannot be simply explained by the change in the rotation, suggesting that the NTM is affected by a sawtooth crash.

Frequency spectrum for 2-unit ECCD case, where $I_{\mathrm{EC}} \sim 70$ kA, is shown in Figs. 1(d)–(f). Discharge condition is the same as the 4-unit ECCD case except the power of EC wave. While sawtooth oscillations appear after the EC wave injection, precursor is not visible and the sawtooth disappears after the turnoff of the EC wave injection. In addition, modulation of the frequency of the $3/2$ NTM is not observed, suggesting no or weak effect of sawtooth crash on the $3/2$ NTM. Profiles of change in electron temperature during a sawtooth crash for the cases of 4-unit ECCD (E45157) and 2-unit ECCD (E45159) are shown in Fig. 2, where temperature difference ΔT_{e} normalized by electron temperature T_{e} before the sawtooth crash is plotted. Sawtooth crash time in these discharges is $t = 6.986$ s and 6.991 s, respectively. As expected, sawtooth amplitude and inversion radius for the 2-unit ECCD are smaller than those for the 4-unit ECCD case. Also, for the 2-unit ECCD case, the location of the inversion radius stays almost unchanged unlike the 4-unit ECCD case. ECE diagnostic shows that the island center of the $3/2$ NTM is located at $\rho \sim 0.4$ in the both cases. Considering the fact that island width of the $3/2$ mode is about 0.1 in ρ, the sawtooth mixing radius reaches close to the inner side of the $m/n = 3/2$ magnetic island for the 4-unit ECCD case, suggesting the possibility that a sawtooth crash affects the evolution of the $3/2$ mode. It is also probable that larger gradient of current profile at $q = 1.5$ for the 4-unit ECCD case can contribute to the suppression of the mode growth.

Temporal evolution of magnetic perturbation in the frequency range of 5.5–13 kHz for the cases of no ECCD, 2-unit ECCD, and 4-unit ECCD is shown in Fig. 3. For the cases of no ECCD and 2-unit ECCD, magnetic perturbation steadily increases in time after the mode onset. No large difference in the onset time of the $3/2$ NTM is observed between the two cases while sawtooth oscillations exist in the latter case. In addition, while the growth rate for the 2-unit ECCD case is two-fold faster than that for the no ECCD case, the amplitude becomes almost the same after $t \sim 10$ s (not shown in Fig. 3). On the other hand, for the 4-unit ECCD case, while the growth rate at initial phase ($\lesssim 5.7$ s) is comparable to the 2-unit ECCD case, the growth saturates and decreases after then. Note that slight increase and subsequent sudden decrease in the mode amplitude at $t = 6.7$ s and 7.0 s in shot E45157 are attributed to a precursor and crash of the sawtooth. The temporal evolution in shot E45157 seems to correlate with the appearance of precursor and the expansion of the inversion radius (See Fig. 1(c)). The value of β_{N} for the 4-unit ECCD case is higher than the other cases by about 6%. The above result shows the compatibility of sawtooth oscillations and a small-amplitude $3/2$ NTM without large confinement degradation, and is expected to be a new operational scenario for NTM control.

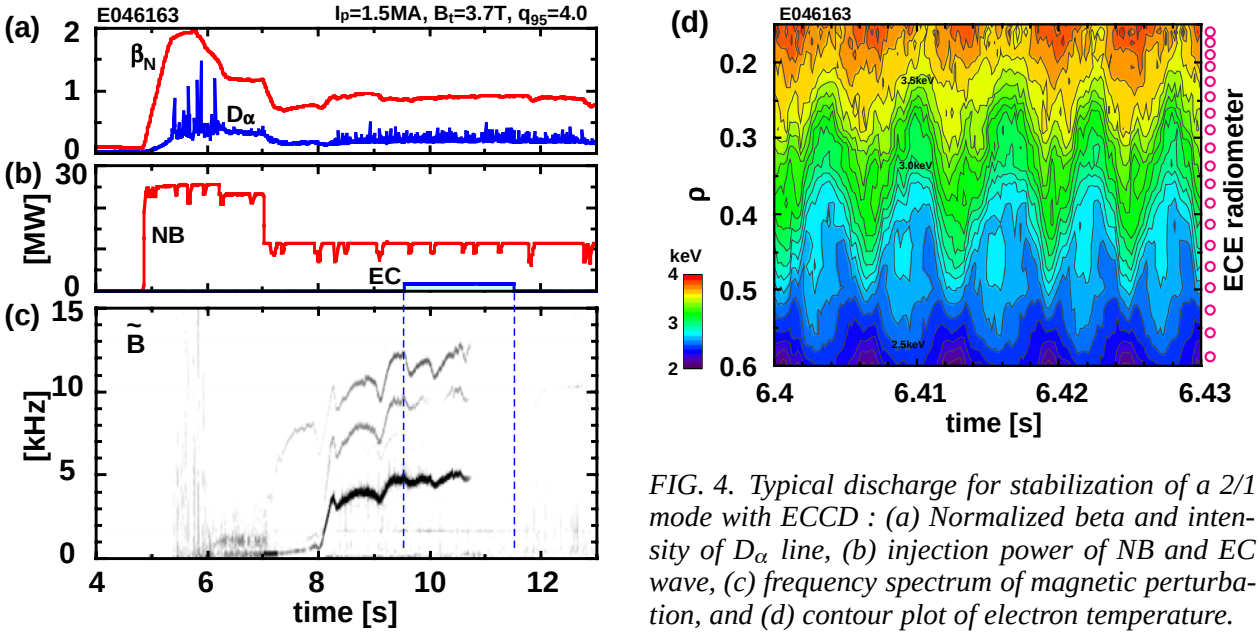

FIG. 4. Typical discharge for stabilization of a 2/1 mode with ECCD : (a) Normalized beta and intensity of D_α line, (b) injection power of NB and EC wave, (c) frequency spectrum of magnetic perturbation, and (d) contour plot of electron temperature.

3. Stabilization of a 2/1 NTM by ECCD at the Mode Location

Suppression of an $m/n = 2/1$ NTM is more important than that of an $m/n = 3/2$ NTM since the $2/1$ NTM causes larger degradation of confinement. For example, in the high-β_p H-mode discharges in JT-60U, degradation of the beta value due to the $2/1$ NTM is $\sim$50% at worst while that due to the $3/2$ NTM is typically $\sim$20%. In JT-60U, two scenarios for NTM suppression have been developed: avoidance of NTM onset through the optimization of pressure and current profiles, and stabilization of NTM by ECCD at the mode rational surface [7]. However, stabilization of a $2/1$ NTM has not been attempted before in JT-60U. This is because the $3/2$ NTM is preferable for understanding the physics of NTM since the effect of the mode on the global parameter is small. Also, the $3/2$ NTM is easier to stabilize because the mode is located at more central regime and thus larger amount of EC-driven current is available under the limited EC wave power.

In JT-60U, stabilization of a $2/1$ NTM has been performed in order to clarify the physics of NTM stabilization. In particular, dependence of the stabilization effect on ECCD location and critical EC wave power required for complete stabilization have been investigated in detail. Typical discharge of an NTM stabilization experiment is shown in Fig. 4. Plasma parameters are as follows: $I_p = 1.5$ MA, $B_t = 3.7$ T, and $q_{95} = 4.0$. By injecting NBs of $\sim$20 MW at $t = 4.8$ s, β_N increases to about 2 ($\beta_p = 1.5$). At $t = 5.75$ s, an $m/n = 2/1$ mode is excited and β_N significantly decreases to ~ 1. Since the frequency of the $2/1$ mode at the onset is low, the mode behavior is not clear from the frequency spectrum in Fig. 4(c). However, the onset can be clearly identified by ECE signals. A contour plot of electron temperature profile at $t = 6.4$ s is shown in Fig. 4(d), where measurement points of ECE radiometer are also indicated. As can be seen in this figure, a flat region is formed at $\rho = 0.4$–0.55, and its width is about 15 cm. It can be also seen that the fluctuations extend far outside the island region. It is interesting to note that temperature inside the island is not completely flat, but small perturbation is observed. Frequency spectra of ECE signals show that higher harmonics of the oscillations mainly originate from the island region. At $t = 7$ s, NB power is reduced and the direction of the NB is changed to the counter direction in order to increase the mode frequency and to accomplish complete stabilization more easily. Shortly after the decrease of NB power, mode frequency starts to increase and reaches about 5 kHz at 9.5 s. Although the value of β_N decreases to about 0.9 in this phase, the $2/1$ mode survives due to the hysteresis characteristics of NTMs that the beta value at the mode

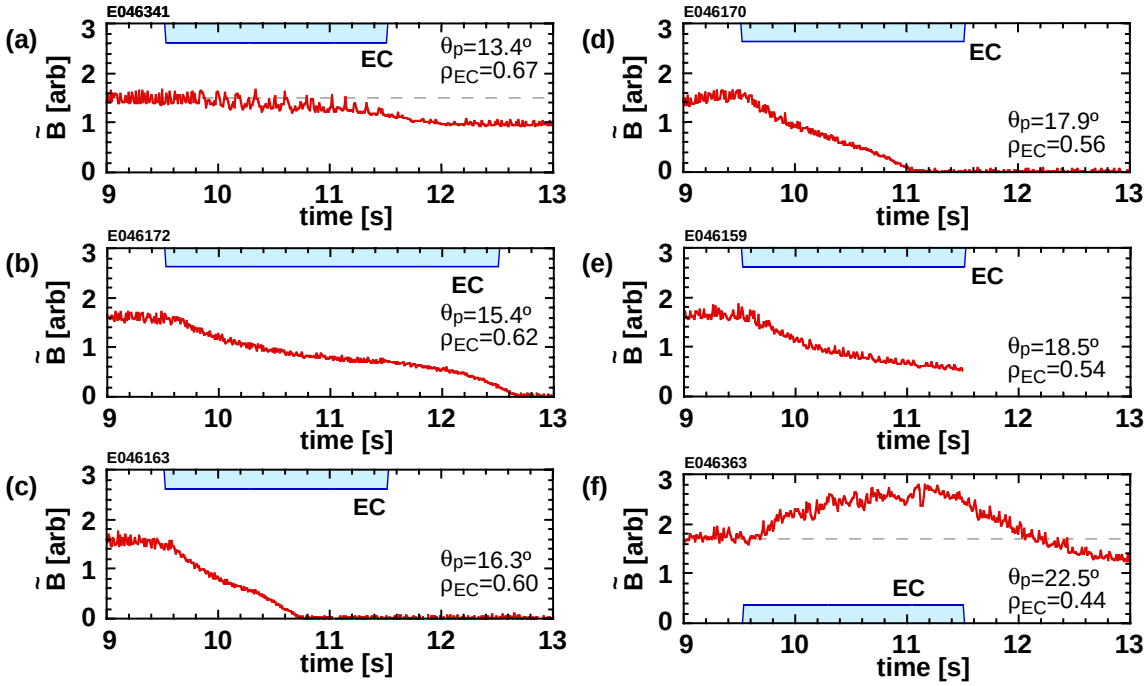

FIG. 5. Temporal evolution of magnetic perturbations for various ECCD locations in $2/1$ mode stabilization experiments. ECCD locations of (a) to (f) are $\rho_{\rm EC}$=0.67, 0.62, 0.60, 0.56, 0.54, and 0.44, respectively.

disappearance is much lower than that at the mode onset (typically the latter is more than twice as large as the former in JT-60U). At $t = 9.5$ s, unmodulated, fundamental O-mode EC wave, whose power $P_{\rm EC}$ is 2 MW, is injected. A ray tracing code shows that the deposition location of the EC wave, $\rho_{\rm EC}$, is 0.6. The $2/1$ mode is completely stabilized at $t = 10.8$ s.

It was reported that for an $m/n = 3/2$ NTM, stabilization effect of ECCD strongly depends on the ECCD location: if the ECCD location is misaligned by about half of the island width, stabilization effect is significantly reduced [4]. To investigate the dependence for a $2/1$ NTM, scan of ECCD location has been performed in detail. Figure 5 shows temporal evolution of magnetic perturbation for various EC wave injection angles. The angle indicated in each figure corresponds to the poloidal injection angle $\theta_{\rm p}$ defined as the depression angle (0° and 90° correspond to horizontal and vertically downward directions, respectively.). Toroidal injection angle is about 20° at all injection angles in Fig. 5. ECCD location calculated with a Fokker-Planck code is also shown in this figure. It can be seen that, as was recognized in the stabilization of a $3/2$ NTM, the stabilization effect strongly depends on the ECCD location: complete stabilization cannot be achieved if the ECCD location is misaligned by about half of the island width (See also Fig. 6(b)). Also, it can be clearly seen that it takes longer time to stabilize the mode if the ECCD location is slightly misaligned. The $2/1$ NTM in Figs. 5(b)–(d) decays in a similar way while the time for complete stabilization is different: rapid decrease just after ECCD, subsequent slowdown, and final rapid decrease. The behavior is qualitatively consistent with that predicted by the modified Rutherford equation. It should be noted that the amplitude at which the final decay starts is similar in these three cases ($\tilde{B} \sim 0.05$). The fact suggests that the marginal island width at which the NTM spontaneous decays is not strongly affected by ECCD location. It was recently reported from cross-machine comparison that for a $3/2$ NTM the marginal island width is proportional to twice the ion banana width [9]. Similar comparison will clarify the physics of the spontaneous decay of a $2/1$ NTM in more detail.

In stabilizing an NTM, the ratio of EC-driven current density $J_{\rm EC}$ to bootstrap current density $J_{\rm BS}$ at the mode rational surface is a measure to evaluate the efficiency of the stabilization. It was demon-

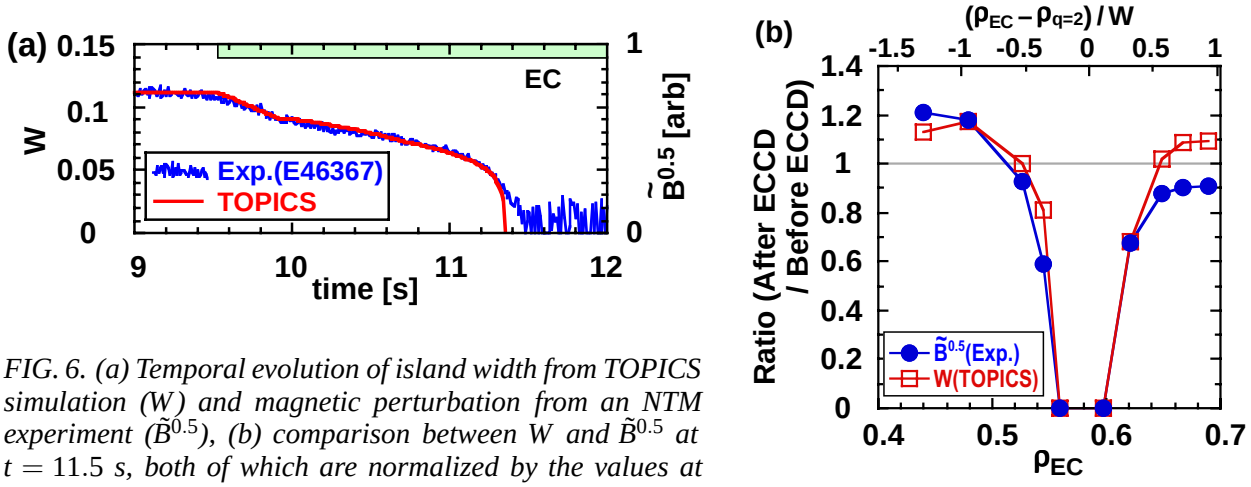

FIG. 6. (a) Temporal evolution of island width from TOPICS simulation (W) and magnetic perturbation from an NTM experiment ($\tilde{B}^{0.5}$), (b) comparison between W and $\tilde{B}^{0.5}$ at $t = 11.5$ s, both of which are normalized by the values at $t = 9.5$ s (just before ECCD).

strated in JT-60U that an $m/n = 3/2$ NTM can be stabilized at $J_{EC}/J_{BS} \sim 1$. Note that the stabilization effect also depends on the width of ECCD profile. In the experimental configuration in this paper, ECCD width is about 0.1 in ρ and comparable to the island width before ECCD. EC-driven current evaluated by a Fokker-Planck code and bootstrap current evaluated by the TOPICS code show that the ratio $J_{EC}/J_{BS} \sim 1$ in shot E46163 (Fig. 5(c)). By further optimizing the EC wave injection angle and setting at $\theta_p = 16.5°$, a $2/1$ mode was completely stabilized only with $P_{EC} = 0.6$ MW, $I_{EC} = 4.8$ kA (Temporal evolution of magnetic perturbation is shown in Fig. 6(a)). The value of J_{EC}/J_{BS} at the mode rational surface is about 0.5, which is the smallest value ever achieved in JT-60U.

In this series of discharges, destabilization effect by misaligned ECCD has been experimentally observed. As shown in Fig. 5(f), magnetic perturbation increases after ECCD when the ECCD location is misaligned by about 0.1 in ρ, which is comparable to the island width. Island width evaluated with ECE diagnostic also indicates that the island width increases by ∼20%. Although the degradation of confinement due to the destabilization itself is not large, mode locking and subsequent large confinement degradation (∼ 25% of the stored energy) were observed during misaligned ECCD in some discharges, showing again that precise adjustment of ECCD location is important.

4. Simulation of NTM Stabilization with the TOPICS Code

Evolution of magnetic island associated with an NTM is described by the modified Rutherford equation (MRE). According to the MRE, temporal evolution of magnetic island is affected by several effects, such as the classical tearing mode effect, the bootstrap current effect, the polarization current effect, and the ECCD effect. Since these terms have different dependence on the magnetic island width, comprehensive analysis including all these terms is important for better prediction of the island evolution.

In JT-60U, the MRE has been combined with a transport code TOPICS, which enables self-consistent analysis of magnetic island evolution. By estimating the undetermined coefficients in the MRE by using experimental data, simulation of the stabilization of a $3/2$ NTM was performed [10, 11]. As described in the previous section, experiments of a $2/1$ NTM stabilization with various ECCD locations and EC wave power have been performed in 2006. The undetermined coefficients for a $2/1$ NTM have been estimated from these experiments. And, by using the same set of the coefficients, comparison of magnetic island width between experiment and TOPICS simulation has been made.

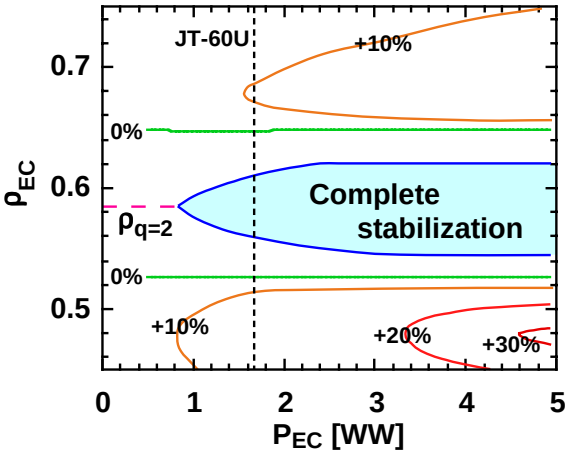

FIG. 7. Contour plot of the increment of magnetic island width as a function of EC wave power and ECCD location.

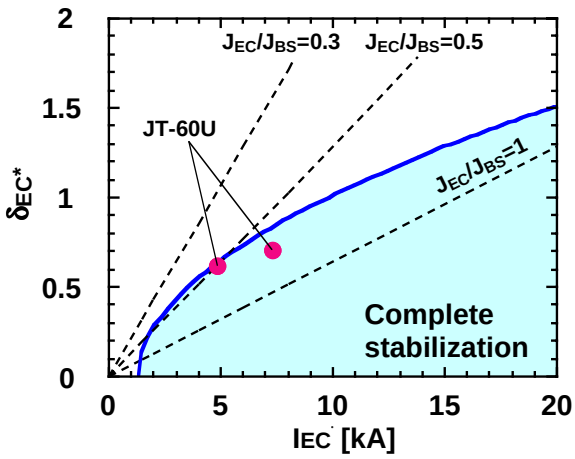

FIG. 8. Contour plot of normalized magnetic island width as a function of total EC-driven current and ECCD width.

Temporal evolution of $\tilde{B}^{0.5}$ as a measure of magnetic island width is shown in Fig. 6(a). In this discharge, a $2/1$ NTM is completely stabilized with one unit of ECCD as described above. Temporal evolution of magnetic island width evaluated by TOPICS simulation, W, is also shown in Fig. 6(a). As can be seen in this figure, the temporal evolution can be well reproduced by the TOPICS simulation by optimizing the combination of the coefficients of the MRE. Figure 6(b) shows W and $\tilde{B}^{0.5}$ at $t = 11.5$ s plotted against the ECCD location (Temporal evolutions in experiments are partially shown in Fig. 5.). In this figure, the values of the vertical axis are normalized by those at $t = 9.5$ s, that is, just before ECCD. The both results show good agreement in that (i) strong stabilization effect appears only when the misalignment is less than about half of the island width, and (ii) destabilization effect appears when the misalignment is comparable to the island width. Note that the destabilization effect for $\rho_{\rm EC} = 0.48$ is larger than that for $\rho_{\rm EC} = 0.70$. One major reason is that $I_{\rm EC}$ decreases with increasing $\rho_{\rm EC}$. Actually, in the simulation in Fig. 6(b), $I_{\rm EC} = 18$ kA for $\rho_{\rm EC} = 0.48$, while $I_{\rm EC} = 7$ kA for $\rho_{\rm EC} = 0.70$ at 1.6 MW injection.

The degree of stabilization and destabilization are affected by input EC wave power as well as the ECCD location. Figure 7 shows a contour plot of the normalized island width as a function of EC wave power and ECCD location. In this simulation, the location of the $q = 2$ surface, $\rho_{q=2}$, is 0.585 in ρ, and full-width at half-maximum (FWHM) of ECCD profile is 0.08 in ρ. Also, current profile is fixed in order to investigate the ECCD effect alone. The profile in Fig. 6(b) corresponds to the dotted line in Fig. 7. As EC wave power is decreased, the region where the NTM can be completely stabilized shrinks and disappears at $P_{\rm EC} = 0.8$ MW in this simulation condition. This indicates that ECCD location must be aligned more accurately when EC wave power is small. On the other hand, the regime of the complete stabilization expands with increasing the EC wave power, but the boundary for the complete stabilization saturates at $\rho_{\rm EC} = 0.54$ and 0.62. Thus, acceptable range of misalignment is about half of the island width even at high EC wave power. In addition, at high EC wave power destabilization effect becomes larger. At $P_{\rm EC} \gtrsim 4.5$ MW, the TOPICS simulation predicts that island width increases by more than 30%. Thus, precise adjustment of ECCD location is important even when abundant EC wave power is available.

Simulations including the temporal change in the current profile have been also performed. In general, the mode location moves in the way that the island escapes from ECCD: mode location shifts outward for $\rho_{\rm EC} < \rho_{q=2}$ and inward for $\rho_{\rm EC} > \rho_{q=2}$. The TOPICS simulations reflecting the exper-

imental conditions show that the shift is about 1 cm. This result is consistent with the experimental observations that the location of island center measured with ECE radiometer, whose channel separation is 2 cm, is almost unchanged. However, at higher EC wave power, the shift of the $q = 2$ surface becomes larger, and this will make the regime of complete stabilization smaller.

The stabilization effect also depends on the width of ECCD profile. In general, narrower ECCD width and larger amount of EC-driven current are preferable if ECCD location is perfectly aligned. To quantitatively evaluate the effect of ECCD width on NTM stabilization, TOPICS simulation including the MRE has been performed. Figure 8 shows the regime for complete stabilization in the space of EC wave power and FWHM of ECCD profile normalized by the island width before ECCD ($\delta^*_{\rm EC}$). In this simulation, ECCD location is on the mode rational surface. As can be seen in this figure, the boundary for complete stabilization is roughly proportional to $I_{\rm EC}/(\delta^*_{\rm EC})^2$, showing that ECCD width has a stronger effect on NTM stabilization than the amount of EC-driven current. Since the ECCD profile is assumed to be a Gaussian shape in these simulations, the peak current density linearly increases with decreasing the ECCD width. As shown in Fig. 8 with dotted lines, larger value of $J_{\rm EC}/J_{\rm BS}$ is required for complete stabilization when ECCD profile becomes wider.

5. Summary

In JT-60U, control of neoclassical tearing modes using ECCD aiming at sustaining a high-beta plasma has been extensively performed. The results in this paper are summarized as follows:

- Evolution of an $m/n = 3/2$ NTM has been suppressed by central co-ECCD with the amount of $\sim 10\%$ of the plasma current. Frequency of the $3/2$ mode is modulated by a sawtooth crash, suggesting that the sawtooth oscillations can affect the evolution of the $3/2$ mode. This result demonstrates the possibility of coexistence of sawtooth oscillations and a small-amplitude $3/2$ NTM, and this scenario is expected to be a new and easy operational scenario for NTM control.
- An $m/n = 2/1$ NTM has been completely stabilized by ECCD at the mode rational surface. The stabilization has been achieved with a small value of $J_{\rm EC}/J_{\rm BS} \sim 0.5$. It has been also demonstrated that complete stabilization can be achieved when the misalignment of ECCD location is less than about half of the island width, and that the mode amplitude increases when the misalignment is comparable to the island width.
- Simulation of the stabilization of an $m/n = 2/1$ NTM has been performed using the TOPICS code combined with the MRE. It has been found that the TOPICS simulations well reproduce the temporal evolution of magnetic island width observed in JT-60U experiments with the same set of coefficients in the MRE. The TOPICS simulation also predicts that ECCD width has a strong effect on NTM stabilization.

References

[1] GREEN, B.J., et al., Plasma Phys. Control. Fusion **45** (2003) 687.
[2] GANTENBEIN, G., et al., Phys. Rev. Lett **85** (2000) 1242.
[3] PRATER, R., et al., in *Fusion Energy 2000* (Proc. 18th IAEA FEC), IAEA-CN-77/EX8/1.
[4] ISAYAMA, A., et al., Plasma Phys. Control. Fusion **42** (2000) L37.
[5] ISAYAMA, A., et al., Nucl. Fusion **43** (2003) 1272.
[6] NAGASAKI, K., et al., Nucl. Fusion **43** (2003) L7.
[7] ISAYAMA, A., et al., Phys. Plasmas **12** (2005) 056117.
[8] ISAYAMA, A., et al., J. Plasma Fusion Res. SERIES **5** (2002) 324.
[9] LA HAYE, R.J., et al., Nucl. Fusion **46** (2006) 451.
[10] HAYASHI, N., et al., J. Plasma Fusion Res. **80** (2004) 605.
[11] NAGASAKI, K., et al., Nucl. Fusion **45** (2005) 1608.